A New DC-DC Converter Linking LCC-HVDC Transmission Networks

Mohamed A. Elgenedy[1], Ibrahim Alhurayyis[1], Ahmad Elkhateb[1], Khaled Ahmed[2] and Kaspars Kroičs[3]

[1] Queen's University Belfast, Belfast, UK.
[2]University of Strathclyde, Glasgow, UK.
[3]Riga Technical University, Institute of Electrical Engineering, Latvia.

E-Mail: m.elgenedy@qub.ac.uk, ialhurayyis01@qub.ac.uk, a.elkhateb@qub.ac.uk, khaled.ahmed@strath.ac.uk, and kaspars.kroics@rtu.lv

Acknowledgements

This publication was made possible by the EPSRC, UK, under Grant ESCROWS EP/T026162/1 and the EUDP European Partnership Development Scheme, DfE, Queen's University Belfast. The statements made herein are solely the responsibility of the authors.

Keywords

«Current-source DC-DC», «DC-DC power converter», «Dual Active Bridge (DAB) DC-DC converter», «IGCT», «Multi-terminal HVDC»

Abstract

Transferring bulk power via high voltage direct current (HVDC) transmission is dominated by line commutated converters (LCC). This is due to the robustness and higher ratings of the thyristors as well as the higher converter efficiency. Nevertheless, most of these transmission networks are point to point. This is due to the challenges of allowing multi-terminal LCC based networks and power reversal. This paper introduces a new dc-dc converter topology that allows connecting two independent LCC networks. The proposed converter is based on insulated gate commutated thyristors (IGCTs). Utilizing IGCTs allow mimicking similar control and performance as in insulated gate bipolar transistor (IGBT) based voltage source dc-dc converters. However, IGCTs have more superior features over IGBTs such as higher efficiency, higher short circuit current and higher power ratings. Detailed analysis and simulations are provided to validate the proposed converter topology, which confirms its potential in connecting HVDC-LCC networks.

Introduction

Point to point high voltage direct current (HVDC) not only utilizing line commutated converters (LCCs) but also voltage source converters (VSCs). Nevertheless, HVDC bulk power transfer is dominated by LCCs [1]. An LCC is a current source converter (CSC) in nature, so naturally, it is fault-tolerant. Moreover, it is based on thyristors which are available not only at low prices but at higher ratings and lower operation losses [1]. On the downside, thyristors control is quite challenging and cannot be turned OFF as an insulated gate bipolar transistor (IGBT), for example [2]. As a result, to reap the rewards of the CSC at medium voltage level, the thyristors are replaced by a controllable combination of an IGBT in series with a diode [3]. This approach is not valid in HVDC, but it can effectively compete with medium voltage VSCs especially in long cables fed motor drives [4], offshore wind farm power collection [5] and multi-phase machine drives application [6].

Several research studies have been considering VSCs for HVDC transmissions [7]-[9]. With fully ON/OFF IGBT switches control, decoupling of the active and reactive power is possible and the overall control is simplified. A game-changing topology for VSC-HVDC is modular multilevel converters (MMC), which can reach very HV levels at lower switching frequencies [10]. But in comparison with

This is a peer-reviewed, accepted author manuscript of the following article: Elgenedy, M. A., Alhurayyis, I., Elkhateb, A., Ahmed, K., & Kroics, K. (2021). A new DC-DC converter linking LCC-HVDC transmission networks. In 2021 23rd European Conference on Power Electronics and Applications (EPE'21 ECCE Europe) IEEE. https://doi.org/10.23919/epe21ecceeurope50061.2021.9570474

LCC, the operation efficiency is lower. Therefore, the power transmitted is lower than LCC-HVDC. Moreover, the used thyristors in LCC-HVDC have higher reliability, higher power ratings and smaller conduction losses than the VSC-HVDC IGBTs [11]-[12]. But, since the thyristors have limited switching frequency (<1kH), large filters are incorporated.

With the development and research kept on going to develop topologies for HVDC bulk power transfer, multi-terminal HVDC networks are also researched. The ultimate goal is to achieve a multi-terminal HVDC network in which the power can be exchanged mutually. Most of these studies are VSC focused on the incorporation of the dual active bridge (DAB) originally proposed by De-Doncker [13]. The main aim is to have high voltage dc-dc converters that enable bi-directional power exchange, voltage stepping up/down and fault isolation [14]-[15]. Additionally, a few attempts have been made in the literature to enable multi-terminal for LCC-HVDC networks [16]-[17], where a thyristor-based dc-dc converter is proposed. The topologies allow connecting two LCC terminals with different voltage level through two thyristor bridges. Hence, a bidirectional power flow is attained. Nevertheless, a complicated control scheme is inevitable based on changing the switching frequency to provide the correct delay angle for the thyristors. In [18], combining the LCC-HVDC with VSC-HVDC is explored. The power reversal is achieved by reversing the current flow in VSCs, but if the power is reversed in LCC, the dc voltage polarity is reversed. Hence the proposed integration in [18] focused on unidirectional power from the LCC. Finally, in [19], a modified DAB topology is adopted to allow LCC-HVDC and VSC-HVDC networks by using passive *LC* tank selected such that the reactive power transfer at rated power transfer is nullified.

This paper proposes a new LCC-DAB dc-dc converter topology based on insulated gate commutated thyristors (IGCTs). The IGCTs are ideal for operation with CSC. Not only they can be turned ON/OFF similar to IGBTs, but also they have reverse blocking capability. Therefore, they combine the best features of the thyristor and the IGBT. Nevertheless, they require complex gate drive circuits with higher power than typical IGBTs [12]. Detailed analysis and simulations are introduced in this paper, aiming to explore the possibility of having a dc-dc converter resembling the well-established VSC based DAB. Hence, multi-terminal networks for LCC-HVDC are enabled. The obtained simulation results and analysis show promising potential for the proposed topology.

Proposed Topology Description

The proposed dc-dc converter topology is depicted in Fig. 1. The topology is formed of two bridges, Bridge-A and Bridge-B. Both bridges are front to front (F2F) connected via an ac-link capacitor C. Both are CSCs fed from LCC- HVDC systems. Therefore, the dc-link inputs I_{dc1} and I_{dc2} for Bridge-A and Bridge-B have fixed polarity. Each bridge is formed of IGCT switches T_i and Q_i (where $i \in \{1, 2, 3, 4\}$) for Bridge-A and Bridge-B, respectively.

In order to allow power transfer between the F2F bridges, the dc-link voltage polarity of each bridge has to be reversed. As a result, the ac-link capacitor is rotated, this can be done by proper switching of the bridges T_i and Q_i IGCT switches. A duty cycle $D = 0.5$ is applied for each bridge switches such that each leg switches are operated in complementary mode. Then, a phase shift angle δ between the bridges generated ac currents is introduced. Therefore, the power can be exchanged between the two bridges (hence, the HVDC networks). Fig. 2 shows the modulation principle of the two bridges when Bridge-B ac current, i_{ac2}, is shifted by an angle δ from Bridge-A ac current, i_{ac1}.

Proposed Topology Operation Analysis

The simplified LCC-DAB converter circuit is illustrated in Fig. 3. In the introduced analysis in this section, only the fundamental component of the square currents i_{ac1} and i_{ac2} waveforms are considered and are denoted i_1 and i_2, respectively.

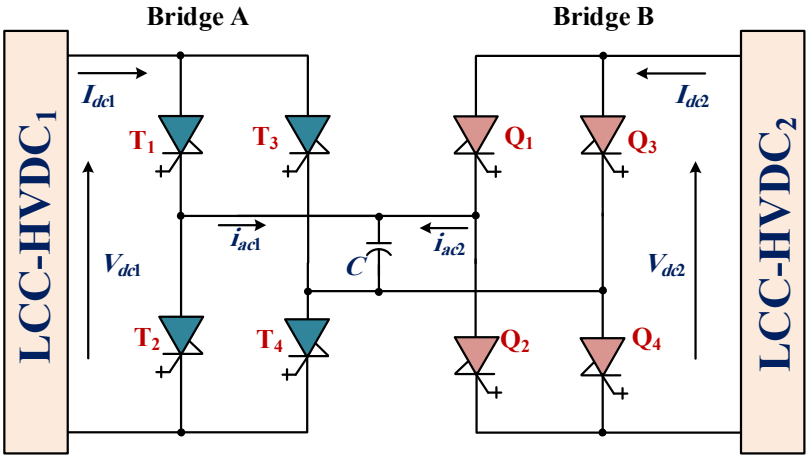

Fig. 1: Proposed dc-dc converter.

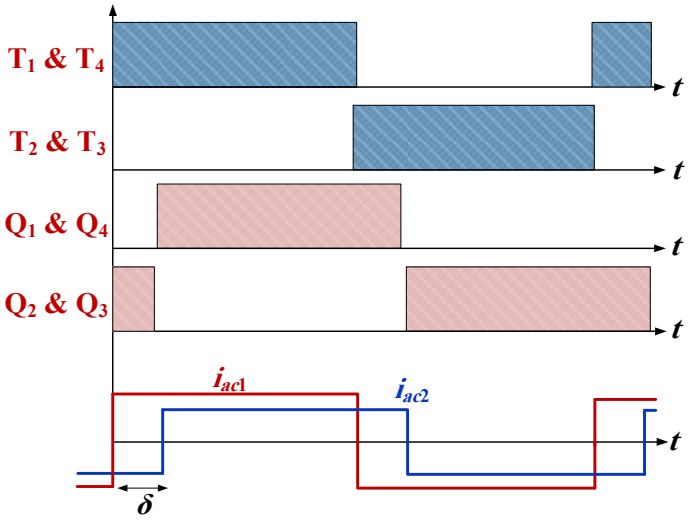

Fig. 2: Proposed LCC-DAB modulation principle.

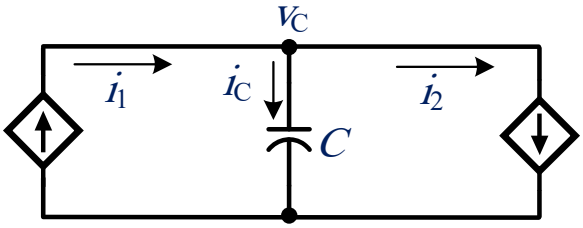

Fig. 3: Simplified LCC-DAB circuit.

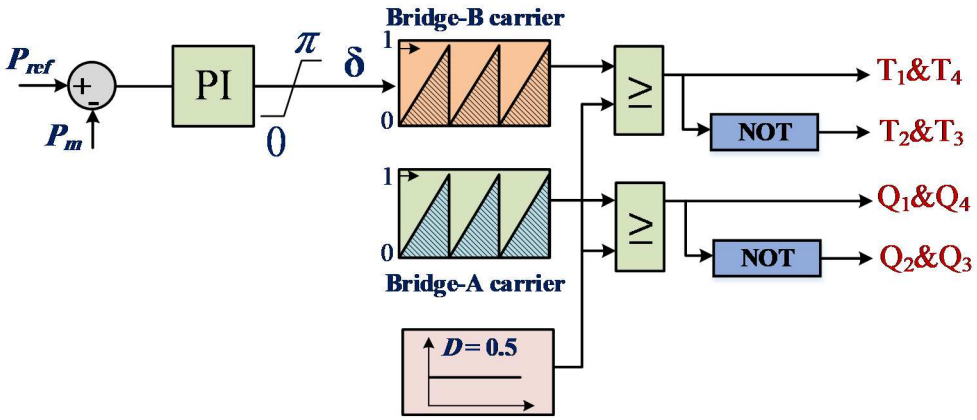

Fig. 4: LCC-DAB phase-shift control principle.

A. Power Transfer

In order to formulate the power transfer equation, the bridges ac currents are represented in phasor form as follows

$$\bar{I}_1 = I_1\angle 0 = I_1 + j0 \quad (1)$$

$$\bar{I}_2 = I_2\angle -\delta = I_2\cos\delta - jI_2\sin\delta \quad (2)$$

where I_1 and I_2 are the peak fundamental ac currents of Bridge-A and Bridge-B, respectively. Also, Bridge-B ac current lags Bridge-A ac current by an angle δ. In this proof without loss of generality, the power is directed from Bridge-A to Bridge-B. The ac capacitor voltage can be expressed as

$$\bar{V}_C = \frac{\bar{I}_C}{j\omega C} \quad (3)$$

where

$$\bar{I}_C = \bar{I}_1 - \bar{I}_2 \quad (4)$$

using (1) and (2) hence

$$\bar{I}_C = (I_1 - I_2\,cos\,\delta) + jI_2\sin\delta \quad (5)$$

therefore

$$\bar{V}_C = \frac{1}{j\omega C}(j(I_2\,cos\,\delta - I_1) - I_2\,sin\,\delta) \quad (6)$$

Assuming lossless bridges and ac-link capacitor (i.e. $P_{dc1} = P_{ac1} = P_{ac2} = P_{dc2} = P$), the power exchanged between bridges can be expressed as follows

$$P = Re\{\bar{V}_C\bar{I}_2^*\} \quad (7)$$

from (2) and (6), the power can be expressed as

$$P = Re\{\frac{1}{j\omega C}(j(I_2\,cos\,\delta - I_1) - I_2\,sin\,\delta)(I_2 + jI_2\,sin\,\delta)\} \quad (8)$$

Simplifying and arranging yields

$$P = \frac{I_1 I_2}{\omega C}sin\,\delta \quad (9)$$

Assuming full square waveform is generated from the dc-link currents, hence

$$I_1 = \frac{2\sqrt{2}}{\pi}I_{dc1} \quad (10)$$

$$I_2 = \frac{2\sqrt{2}}{\pi}I_{dc2} \quad (11)$$

substituting (10) and (11) into (9) the power transfer equation in terms of the dc-link currents will be

$$P = \frac{8I_{dc1}I_{dc2}}{2\pi^3 fC}sin\,\delta \quad (12)$$

where f is the ac-link frequency at which the switches will generate the ac-currents.

As illustrated in (12), the power amount and direction can be exchanged between both bridges while keeping the ac link frequency constant. Similar to conventional VSC based DAB, introducing a phase-shift between the created bridges ac currents leads to a controllable power transfer. As a result, the proposed dc-dc converter resembles a conventional VSC-DAB which allow simpler control rather than the frequency control proposed in [16]. The control scheme based on varying the shift angle δ is illustrated in Fig. 4.

B. AC-link capacitor voltage and current

Considering the polarity of the currents illustrated in Fig. 1, a generic capacitor ac voltage and current are depicted in Fig. 5. Analyzing the voltage waveform yields three consecutive intervals as follows:

- Interval $[t_0,\ t_1]$, the capacitor voltage $v_C(t)$ is expressed as

$$v_C(t) = \frac{\delta T_s}{2C} i_C + v_C(t_0) \tag{13}$$

where $T_s = 1/f$. Hence, $v_C(t_1)$ can be expressed as

$$v_C(t_1) = \frac{\delta T_s}{2C} i_C + v_C(t_0) \tag{14}$$

- Interval $[t_1,\ t_2]$, the capacitor voltage $v_C(t)$ is expressed as

$$v_C(t) = \frac{(1-\delta) T_s}{2C} i_C + v_C(t_1) \tag{15}$$

- Similarly, $v_C(t_3)$ can be obtained from expressing $v_C(t)$ in the interval $[t_2,\ t_3]$ as follows

$$v_C(t_3) = \frac{\delta T_s}{2C} i_C + v_C(t_2) \tag{16}$$

Due to waveform symmetry, it can be noted that

$$v_C(t_3) = -v_C(t_1) \tag{17}$$

and

$$v_C(t_2) = -v_C(t_0) \tag{18}$$

Re-arranging and solving for $v_C(t_0)$ yields

$$v_C(t_0) = \frac{T_s i_C}{4C}\ (1 - 2\delta) \tag{19}$$

As a result of this studied case, the maximum capacitor voltage $v_C(t_2)$ is obtained. Therefore, the stresses and the maximum capacitor voltage are determined. Moreover, there are three distinct cases, as shown in Fig. 6, depending on the dc-link currents level. Fig. 6a shows the capacitor current and voltage when $I_{dc1} > I_{dc2}$, where the maximum capacitor voltage appears at the beginning of the intervals $[t_0,\ t_1]$ and $[t_2,\ t_3]$. This particular case is reversed when $I_{dc1} < I_{dc2}$ as illustrated in Fig. 6b. Finally, Fig. 6c shows the waveforms when $I_{dc1} = I_{dc2}$.

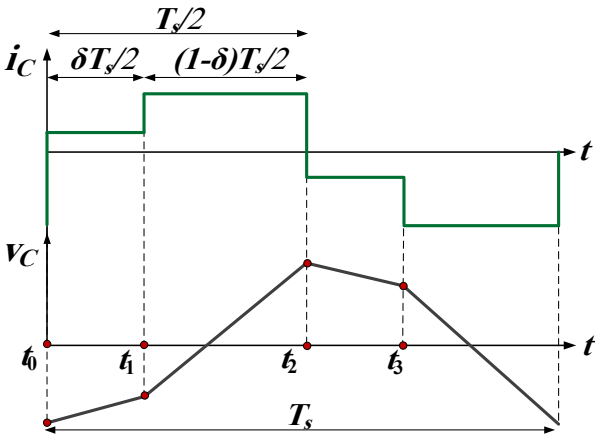

Fig. 5: Generic capacitor voltage waveform.

Proposed Topology Operation Analysis

The proposed LCC-DAB converter, shown in Fig. 1, is MATLAB/SIMULINK simulated. The simulation parameters are given in Table I. In order to simplify the simulations, stiff dc current sources are utilized.

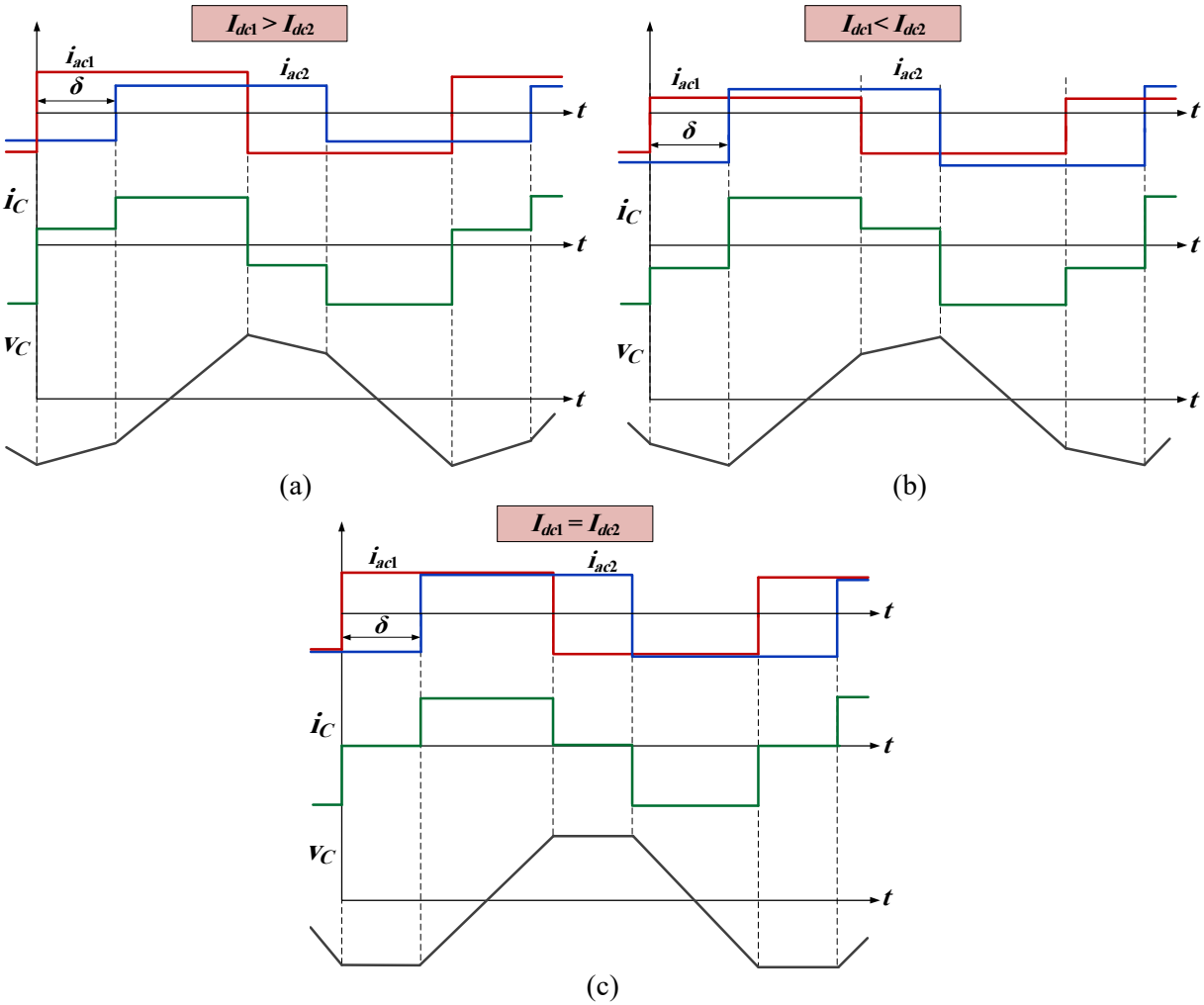

Fig. 6: Variation of capacitor voltage waveform based on the difference in dc-link currents.

A. Simulating the dc-link currents level effect on the ac-link capacitor voltage

At fixed phase shift angle $\delta = \pi/2$ Bridge-A dc-link current is fixed at 100A while Bridge-B dc-link current is varied as illustrated in Table I.

Table I: Simulation Parameters

dc-Link current at Bridge-A (fixed), I_{dc1}	100A
dc-Link current at Bridge-B (varied), I_{dc2}	(75, 100, 125) A
C	150µF
$f\left(\frac{1}{T_s}\right)$	150Hz
δ	$\pi/2$

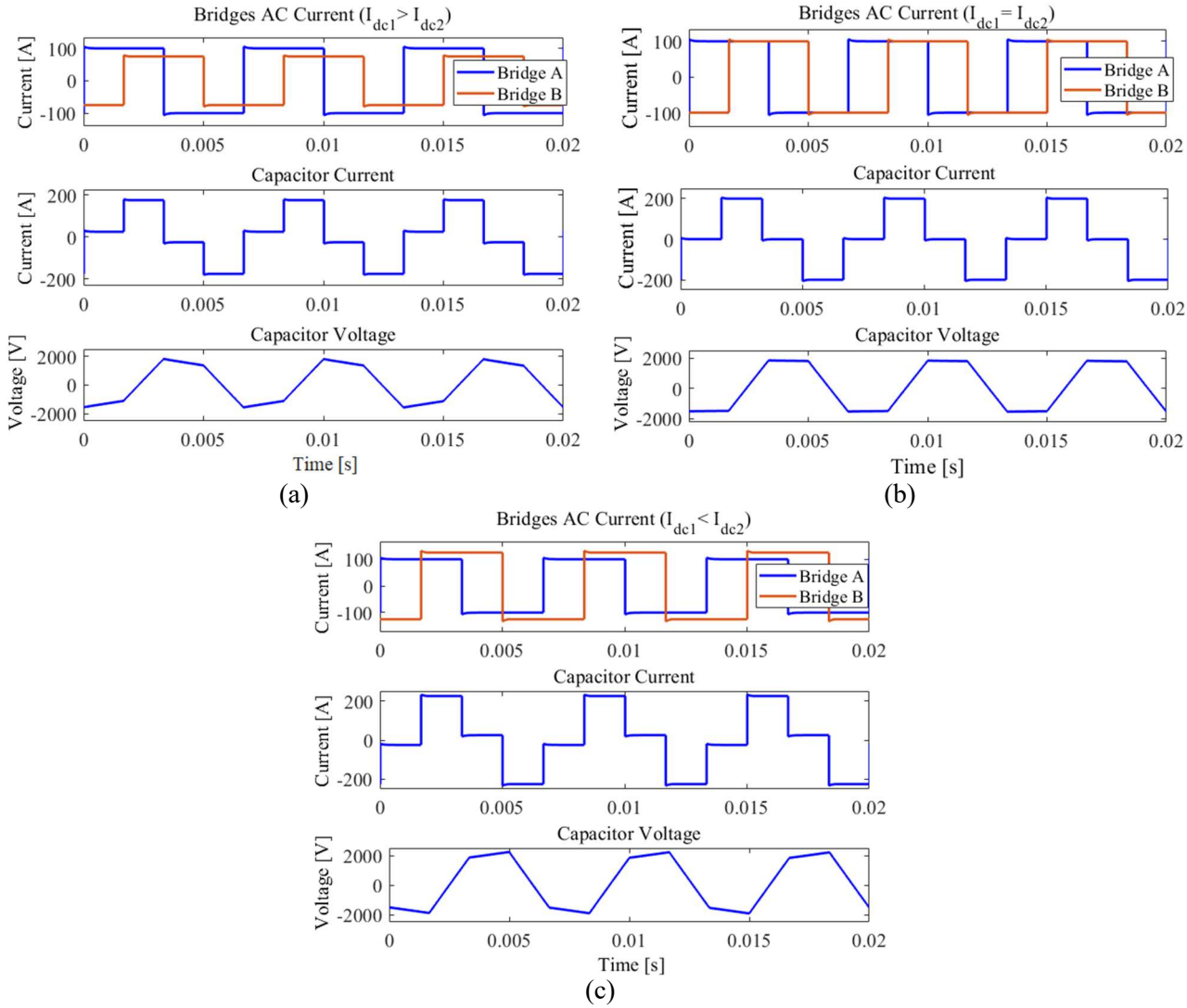

Fig. 7: Simulation results when varying the dc-link current levels. (a) $I_{dc1} > I_{dc2}$. (b) $I_{dc1} = I_{dc2}$. (c) $I_{dc1} < I_{dc2}$.

Fig. 7 show the obtained simulations when Bridge-B dc-link current has three different values 75 A, 100 A and 125A. In Fig. 7a, $I_{dc1} > I_{dc2}$, hence the resultant capacitor voltage waveform has no peak plateau similar to the case of $I_{dc1} = I_{dc2}$ (shown in Fig. 7b), instead it has a peak voltage at each raising and falling edge of I_{ac1}. In contrast, the peak capacitor voltage appears at each raising and falling edge of I_{ac2} as shown in Fig. 7c.

B. Simulating the power exchange control scheme

As shown in (12), controlling the amount and the direction of power exchange can be effectively controlled by the phase-shift angle δ while keeping other variables constant. If $0 < \delta \leq \pi/2$, the power flows from Bridge-A to Bridge-B, but it flows from Bridge-B to Bridge-A when $\pi/2 < \delta \leq \pi$. The control scheme illustrated in Fig. 4 shows the methodology of power flow control. With of $I_{dc1} = I_{dc2} =$ 100A, and the same parameters in Table I the maximum power (at $\delta = \pi/2$) is $P_{max} =$ 86kW. Assuming the positive power direction is from Bridge-A to Bridge-B, the simulation scenario for the controller reference power P_{ref} is as follows:

- Interval I: $P_{ref} = P_{max}$, for $0 \leq t < 0.5$s,
- Interval II: $P_{ref} = 0.5P_{max}$, for $0.5 \leq t < 1.5$s,
- Interval III: $P_{ref} = -0.5P_{max}$, for $t \geq 1.5$s.

The controller will determine and assign the correct phase-shift angle such that the error between the measured power, P_m, and the reference power, P_{ref}, is nullified. As expected from (12) and shown in Fig. 8, the controller will assign $\delta = \pi/2$ to allow the maximum power to transfer in interval I. In interval II, $\delta = \pi/6$ in order to transfer half the power. Therefore, in interval III, $\delta = -\pi/6$ to allow half power transfer from Bridge-B to Bridge-A. Finally, Fig. 9 shows the created ac currents at each bridge as well as the resultant capacitor current and capacitor voltage during the period of power reversal. During interval II, the ac current of Bridge-B lags the ac current of Bridge-A by δ, while during power reversal the controller force the ac current of Bridge-A to lag the ac current of Bridge-B by δ hence the power is reversed in interval III.

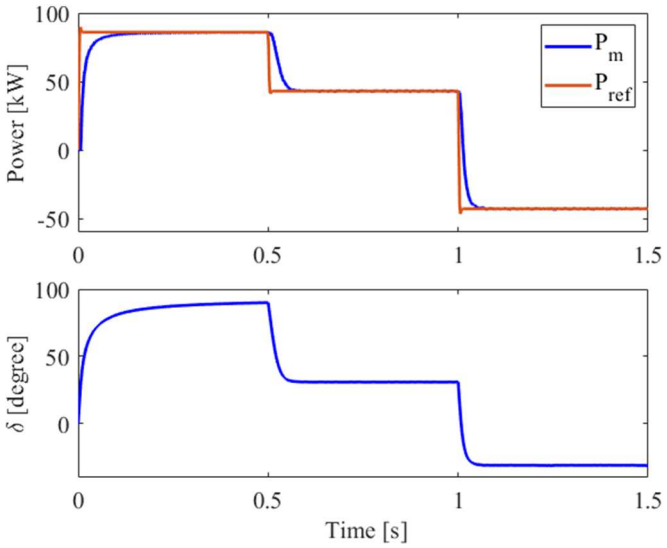

Fig. 8. Simulation results when varying the power transfer amount and direction.

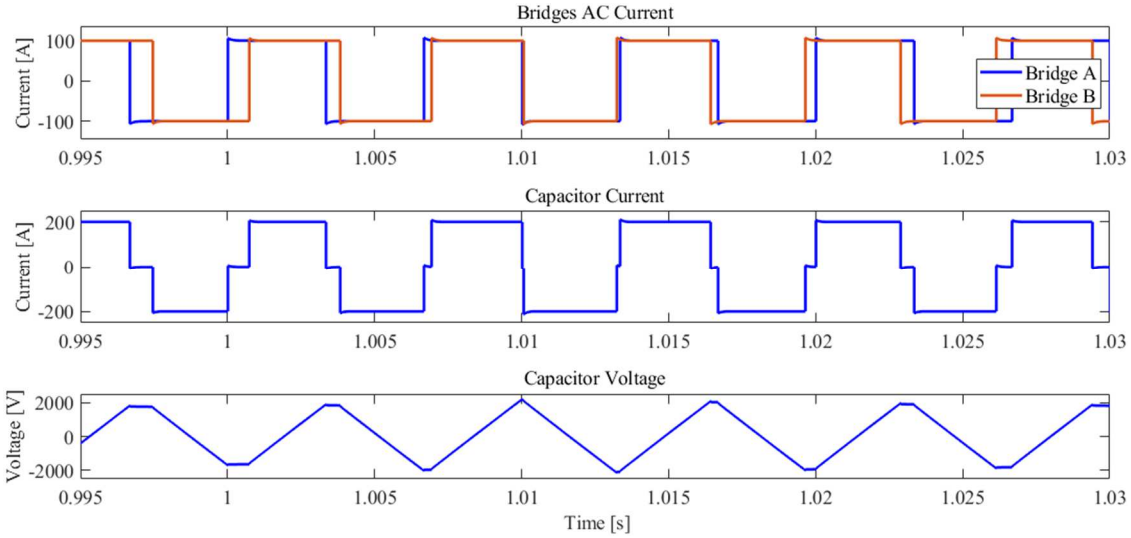

Fig. 9. Simulation results for the capacitor voltage and current during the power reversal period.

Conclusion

This paper proposed a new dc-dc converter to enable the possibility of connecting two LCC-HVDC systems with different dc-link current levels. The proposed converter adopts IGCT switches along with an ac-link capacitor for interfacing both networks. The ac-link capacitor will rotate its polarity voltage, enabling power transfer between the terminal LCC-HVDC networks. Adopting IGCTs in the proposed converter allows simpler control, similar to VSC-DAB. Moreover, the main advantages of IGCTs over IGBTs with series diodes are the inherited reverse blocking capability, lower conduction losses, lower price, lower footprint and higher reliability. On the downside, the gate drive for IGCTs are complex and require higher powers than typical IGBT drive power (about ten times higher). The proposed converter is analyzed, and it is proved that the power transfer can be controlled by only controlling the phase-shift angle between the created ac-link currents. The proposed converter is simulated under different dc-link current levels along with bidirectional power flow. The obtained results confirm the viability of the proposed converter, which allow possible LCC-HVDC networks connection.

References

[1] Barker et al., *HVDC: Connecting to the Future*. Paris, France: Alstom Grid, 2010.

[2] R. E. Torres-Olguin, M. Molinas, and T. Undeland, "Offshore wind farm grid integration by VSC technology with LCC-based HVDC transmission," *IEEE Trans. Sustainable Energy,* vol. 3*,* no. 4, pp. 899-907, 2012.

[3] M. A. Elgenedy, A. Abdel-Khalik, A. Elserougi, S. Ahmed, and A. M. Massoud, "Sinusoidal pwm modulation technique of five-phase current-source-converters with controlled modulation index," in *2014 IEEE 23rd International Symposium on Industrial Electronics (ISIE)*, 2014, pp. 655-660.

[4] M. A. Elgenedy, A. S. Abdel-Khalik, A. M. Massoud, and S. Ahmed, "Indirect field-oriented control of five-phase induction motor based on spwm-csi," in *2014 International Conference on Electrical Machines (ICEM)*, 2014, pp. 2101-2106.

[5] M. A. Elgenedy, A. Abdel-Khalik, A. Elserougi, S. Ahmed, and A. M. Massoud, "A new five-phase to three-phase back-to-back current source converter based wind energy conversion system," in *2013 7th IEEE GCC Conference and Exhibition (GCC)*, 2013, pp. 193-198.

[6] M. A. Elgenedy, A. A. Elserougi, A. S. Abdel-Khalik, A. M. Massoud, and S. Ahmed, "A space vector pwm scheme for five-phase current-source converters," *IEEE Trans. Ind. Electron.,* vol. 63*,* no. 1, pp. 562-573, 2016.

[7] N. Flourentzou, V. G. Agelidis, and G. D. Demetriades, "VSC-based HVDC power transmission systems: An overview," *IEEE Trans. Power Electron.,* vol. 24*,* no. 3, pp. 592-602, 2009.

[8] A. Egea-Alvarez, F. Bianchi, A. Junyent-Ferre, G. Gross, and O. Gomis-Bellmunt, "Voltage control of multi-terminal VSC-HVDC transmission systems for offshore wind power plants: Design and implementation in a scaled platform," *IEEE Trans. Ind. Electron.,* vol. 60*,* no. 6, pp. 2381-2391, 2013.

[9] D. Van Hertem and M. Ghandhari, "Multi-terminal vsc hvdc for the european supergrid: Obstacles," *Renewable and Sustainable Energy Reviews,* vol. 14*,* no. 9, pp. 3156-3163, 2010.

[10] A. Lesnicar and R. Marquardt, "An innovative modular multilevel converter topology suitable for a wide power range," in *IEEE Bologna Power Tech Conference Proceedings*, 2003.

[11] R. Zeng, B. Zhao, T. Wei, C. Xu, Z. Chen, J. Liu*, et al.*, "Integrated gate commutated thyristor-based modular multilevel converters: A promising solution for high-voltage dc applications," *IEEE Ind. Electron. Mag.,* vol. 13*,* no. 2, pp. 4-16, 2019.

[12] B. Zhao, R. Zeng, Z. Yu, Q. Song, Y. Huang, Z. Chen*, et al.*, "A more prospective look at igct: Uncovering a promising choice for dc grids," *IEEE Ind. Electron. Mag.,* vol. 12*,* no. 3, pp. 6-18, 2018.

[13] R. W. A. A. D. Doncker, D. M. Divan, and M. H. Kheraluwala, "A three-phase soft-switched high-power-density dc/dc converter for high-power applications," *IEEE Trans. Ind. Applicat.,* vol. 27*,* no. 1, pp. 63-73, 1991.

[14] G. P. Adam, I. A. Gowaid, S. J. Finney, D. Holliday, and B. W. Williams, "Review of dc-dc converters for multi-terminal HVDC transmission networks," *IET Power Electronics,* vol. 9*,* no. 2, pp. 281-296, 2016.

[15] I. Alhurayyis, A. Elkhateb, and D. J. Morrow, "Isolated and non-isolated dc-to-dc converters for medium voltage dc networks: A review," *IEEE Journal of Emerging and Selected Topics in Power Electronics,* pp. 1-1, 2020.

[16] D. Jovcic, "Bidirectional, high-power dc transformer," *IEEE Trans. Power Delivery,* vol. 24*,* no. 4, pp. 2276-2283, 2009.

[17] D. Jovcic and B. T. Ooi, "Developing dc transmission networks using dc transformers," *IEEE Trans. Power Delivery,* vol. 25*,* no. 4, pp. 2535-2543, 2010.
[18] R. E. Torres-Olguin, A. Garces, M. Molinas, and T. Undeland, "Integration of offshore wind farm using a hybrid hvdc transmission composed by the pwm current-source converter and line-commutated converter," *IEEE Trans. Energy Conversion,* vol. 28*,* no. 1, pp. 125-134, 2013.
[19] M. A. Elgenedy, K. H. Ahmed, A. A. Aboushady, and I. Abdelsalam, "DC–DC converter concept allowing line commutated converters and voltage source converters based HVDC systems connectivity," *IET Power Electron.*, vol. 13, no. 15, pp. 3294-3304, 2020.